International Journal of Applied Engineering Research ISSN 0973-4562 Volume 10, Number 24 (2015) pp 44315-44325
© Research India Publications. http://www.ripublication.com

Investigation on Vibration Excitation Behavior of an Elastically Mounted Circular Cylinder at Different Interference Conditions

K. Karthik Selva Kumar*,
Department of Mining Machinery Engineering, Indian School of Mines, Dhanbad Jharkhand
kksk88@gmail.com

L. A. Kumaraswamidhas,
Department of Mining Machinery Engineering Indian School of Mines, Dhanbad Jharkhand
lakdhas1978@gmail.com

Abstract
In order to study the fluid flow characteristics and possibilities of suppressing the flow induced vibration excitation in an elastically mounted circular cylinder at different interference conditions, a numerical investigation is performed on a range of longitudinal gap ratios ($2.0 \leq L/D \leq 4.0$) and transverse gap ratios ($2.0 \leq T/D \leq 4.0$) between the cylinders, arranged in tandem and staggered configuration. In this paper a two dimensional computational simulation using Finite Element Method based on Arbitrary Lagrangian-Eulerian (ALE) formulation is performed, with the time integration being carried out by the predictor-corrector method to identify the fluid flow characteristics. Along with that the effects of vortex shedding from the elastically mounted circular cylinder and the fluid dynamic forces acting on the adjacent cylinders were also examined. The observed results of fluid flow characteristics around the elastically mounted circular cylinder are validated with the results of previous studies. Which shows that among all the cylinder arrangements at different spacing ratios, the fluid flow characteristics of elastically mounted circular cylinder in staggered arrangement with two interfering cylinders in upstream conditions, the oscillatory amplitude ratio (A/D=0.250) is found to be minimum at the lock-in regime ranging between ($8.5 \leq V_r \leq 21.5$).

Keywords: Flow Induced Vibration, Vortex Shedding, Tandem Arrangement, Staggered Arrangement, Vibration Amplitude.

Introduction

In the recent years, the study on fluid flow characteristics and its induced vibration has drastically increased in various fields of engineering (Aeronautics, Automobiles, power plants, Buildings, Marine Structures i.e. off shore platforms, etc) and non-engineering applications (Medical applications i.e. flow characteristics of blood vessels). The vibration induced by the fluid flow can be classified according to the nature of the fluid structure interaction, as shown in the following table. I The fluid-flow is broadly classified into three, i.e. internal, external and free shear flow. The present study is about the FIV due to the external flow of fluid over the bluff bodies, i.e. circular, square or the rectangular cylinders. Basically interaction between the fluids and the structures is more of a complex phenomenon to study. Shiels et al, (2001) found out that the FIV of an elastically constrained 2-D circular cylinder has become a significant problem in studying the interaction between the fluids and structures. For these types of problems, Cheng & Zhou (2008) suggested the novel surface perturbation technique to control the factors which are involved in the fluid-structure interactions such as vortex shedding, flow-induced vibrations and vortex-induced noises. From the view of various researchers, some possible sources for the FIV and its analyzing techniques are stated below. The FIV is developed due to an alternating low-pressure, caused by the vortex shedding, behind a submerged cylinder, (Hyun-Boo Lee, et al (2013)). From the studies of Pettigrew et al (1998), it can be identified that the occurrences of vibration induced in the tube bundles by the cross flow is mainly due to the fluid elastic instability.

TABLE.1. Mechanism causing vibration due to the nature of fluid-structure interaction. (K.Karthik Selva Kumar & L.A.Kumaraswamidhas (2014))

MECHANISM CAUSING VIBRATION			
1.	Additional added masses	*8.*	Galloping and flutter
2.	Inertial coupling effect	*9.*	Induced vibration due to fluid elastic instability
3.	Instability due to parallel flow	*10.*	Multi-phase buffeting
4.	Induced vibration due to turbulence	*11.*	Acoustic resonance
5.	Induced vibration due to ocean wave	*12.*	Hydraulic transients
6.	Sonic fatigue	*13.*	Environmental excitation
7.	Induced vibration due to vortex shedding	*14.*	Transmitted mechanical vibration

Ajith Kumar and Gowda (2006), Korkischko and Meneghini (2010) suggested that the total number of cylinders and its arrangements is one of the parameters which had significant impact on the induced vibration due to fluid flow. Kang et al., (2003), proposed an axial-flow-induced vibration model to evaluate the sensitivity to spring stiffness on the FIV of the bluff bodies. The important parameters of the heat exchangers to withstand the FIV are damping, mass per unit length, mass ratio, etc. which must be significantly evaluated at the stage of designing, (Gelbe et al, (1995)). Ostanek and Thole (2012) investigated the near wake flow developed through the arrays

of staggered pin fins in a heat exchanger. Zhou (2003) experimentally investigated the flow behind three side-by-side circular cylinders using different techniques, including Particle Image Velocimetry, Hot-Wire Anemometry, Laser-Illuminated Flow Visualization and Laser Doppler Anemometry. Biswas and Ahamed (2001) investigated the self-excited lateral vibration of a pipe due to an internal fluid flow and also applied an integral minimum principle of Pontryagin to analyze the optimum flow velocity for lesser pipe vibration i.e. to maximize the fluid transport efficiency whereas, it is important to maximize the flow velocity while minimizing the lateral vibration of the pipe. Perotin and Granger (1998) stated that the dynamic behavior of the tube equipped with all the linear and non-linear supports were gathered from an identified turbulent excitation, which provides a highly satisfactory validation for the regularized inverse identification process. Sang-Nyung Kim and Yeon-Sik Cho (2004) employed a mode frequency analysis, which involves subroutine of Structural Routine in ANSYS to carry out the analysis of the natural frequency and relative amplitude of the tube. Using numerical and experimental analysis K.Karthik Selva Kumar & L.A.K Dhas (2014 & 2015) investigated the vibration excitation behavior of circular and square section at different orientation. Jubran et al. (1998) applied a newly developed joint time-frequency analysis techniques (JTFA) and in particular, the modulated Gaussian wavelet to identify the characteristics of the FIV of an elastically mounted single cylinder subjected to cross flow. Kumar et al. (2008) analyzed the flow-induced oscillations of a square section under interference conditions using a data-mining tool called 'decision tree'. K.Karthik Selva Kumar, et al. (2014) analyzed induced vibration excitation of a circular cylinder at different interference conditions using a data-mining tool called 'SPSS'. Wu, et al. (2007) investigated the high-frequency perturbation effects on the performance, to suppress the FIV in the bluff bodies. The component failures due to excessive FIV continue to affect the performance and reliability of the equipments; such failures are very costly in terms of repairs which lead to loss of production (Pettigrew, et al (1998)). In this study, a numerical analysis is done for the suppression of flow-induced vibration excitation in an elastically mounted circular cylinder at different interference conditions that are analyzed and validated with the previous result.

Geometry of the Model

The study on interaction between the fluids and structures is a complicated phenomenon. The present study is about the flow-induced vibration excitation in an elastically mounted circular cylinder at different interference conditions. The schematic representation of an elastically mounted circular cylinder employed for the two dimensional flow simulations along with the basic parameters and applied boundary conditions are shown in Fig 1. Similarly, the elastically mounted circular cylinder model is analyzed at different interference conditions. Where, the (m) represents the mass of the cylinder, (*k*) represents the stiffness and (*c*) represents the damping coefficient. The model represents the dynamics of a simple structure at single vibration mode, most likely the fundamental one. This single degree of freedom (SDOF) system is allowed to oscillate the cylinder in cross flow as shown in the Fig.1, which is perpendicular to the flow that travels from left to right. The spring constant (k) and mass (m) are chosen according to the structural resonance corresponding to a particular Reynolds number, $Re = UD/\nu$ of known value. Where, U represents the free stream velocity, the cylinder diameter is D and υ is the kinematic viscosity.

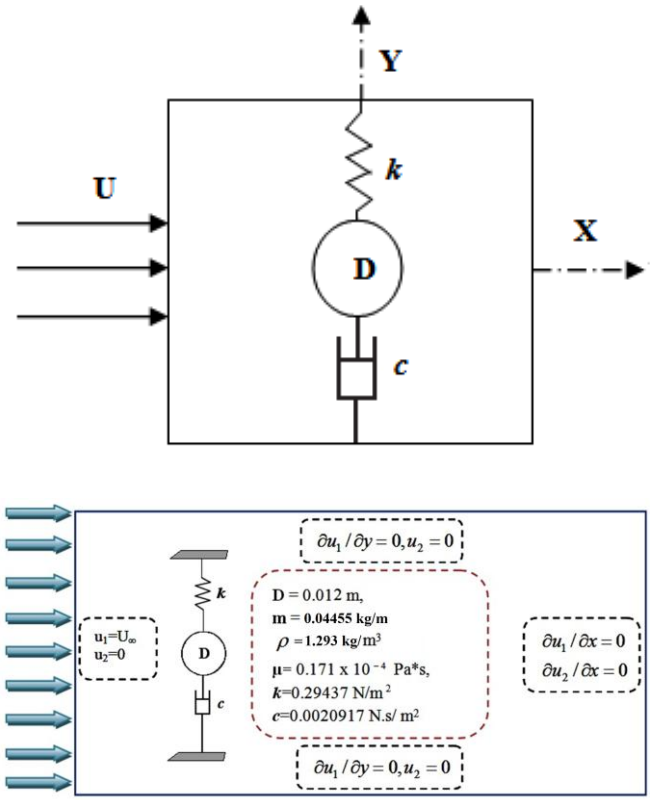

Fig 1: (a) Geometry of elastically mounted circular cylinder model in cross-flow (b) Boundary condition with basic parameters.

Computational Analysis

A. Governing equation:

The aim of the computational study is to predict the vibration response of the cylinder arranged in different interference condition. Where an ALE formulation based Finite Element Method is employed to simulate the interaction of fluid flow with elastically mounted circular cylinder at different interference conditions. In turn, the ALE formulation is based on the mixed standpoint Eulerian and classical Lagrangian descriptions. The Navier-Stokes equations based on ALE formulation is written as:

$$\frac{\partial u_i}{\partial x_i} = 0, \tag{1}$$

$$\rho \frac{\partial u_i}{\partial t} + \rho(u_j - \hat{u}_j)\frac{\partial u_i}{\partial x_j} = \frac{\partial \tau_{ij}}{\partial x_j} + F_i, \tag{2}$$

Where the density of the fluid is ρ, u_i is the flow velocity, $\hat{u}_i$ is considered being the motion mesh velocity, τ_{ij} is the stress tensor, F_i is force exerted from the cylinder. Apart from that, the convection velocity is replaced with relative velocity $(u_i - \hat{u}_i)$ to the mesh velocity $\hat{u}_i$. The stress tensor (τ_{ij}) is written as

$$\tau_{ij} = -p\delta_{ij} + \mu\left(\frac{\partial u_i}{\partial x_j} + \frac{\partial u_j}{\partial x_i}\right), \quad . (3)$$

in which p represents the pressure and μ represent the dynamic viscosity. In this study, the Shear Stress Transport (SST) k-ω turbulence model (Menter model) is employed for modeling the turbulence. A streamline upstream wind method [12], is applied to the ALE based Navier-Stokes equation with bilinear quadrilaterals for velocities and piecewise constants for pressure to obtain the finite element equations which is written as follows,

$$Ma + N(\mathcal{V} - \hat{\mathcal{V}})\mathcal{V} - Gp = F, \quad (4)$$

$$G^t \mathcal{V} = 0, \quad . (5)$$

where **M** represents the mass matrix, **G** accounts for the Gradient matrix**, N** $(\mathcal{V} - \hat{\mathcal{V}})$ for the convection and viscosity, **a** for the acceleration vector, $\mathcal{V}$ represents the material velocity vector, $\hat{\mathcal{V}}$ represents the mesh velocity vector, the pressure vector is p, and the force vector is represented as F**,** where, M, N and G are time dependent. Whereas, at each consecutive time-step the boundary grid points are given by an analytical solution of motion equation for the structures and the inner grid points were generated by solving the Poisson equation. The numerical model of the bluff body with boundary condition is shown in the Fig.1 and the motion equation of the structures is expressed in eqn.6. The software package, FLUENT, has been used to perform the flow simulations. When the flow passed the elastically mounted circular cylinder at certain velocity range, an unsteady pressure fluctuation is acting on its surface as a result of vortex shedding, causing the bluff bodies to oscillate in the y-direction. To obtain the flow field predictions with the moving boundary of the elastically mounted cylinder, a User Defined Function (UDF) is written in C language. The objective of this UDF is to communicate with FLUENT to determine the motion of the SDOF system using the equation of motion:

$$F_y = m\frac{d^2y}{dt^2} + c\frac{dy}{dt} + ky \quad (6)$$

The UDF calculates the values of y in response to the fluid loading, at every time step. This is performed by rearranging the eqn. (6) to give the instantaneous change in velocity and the lift force coefficient C_L are defined as

$$dy' = \frac{(F_y - Cy' - ky)}{m}dt \quad . (7)$$

$$C_L(t) = \frac{2F_y(t)}{\rho U^2 D} \quad (8)$$

Where F_y is the sum of the pressure and viscous forces on the cylinder boundary in cross flow direction; the fluid force acting upon the cylinder are computed the resulting velocity is calculated using the eqn. (8) being interpreted by FLUENT to update the vertical position of the cylinder boundary. Where, FLUENT re-meshes the computational domain in response to the new position of the boundary at each time step.

B. Problem description and mesh system

In the article, an elastically mounted circular cylinder, each of diameter D=14mm, is analyzed with different interference cylinders arranged symmetrically with respect to the Cartesian coordinates at Re=1000. The longitudinal and transverse spacing ratio between the cylinders varies from L/D=2.0,3.0,4.0 and T/D = 2.0, 3.0, 4.0 respectively. The schematic representation of the computational area is shown in the Fig.1 (b) along with the boundary conditions, where the entire computational area is defined as $\Omega = (-20D, 50D) * (-30, 30)$. Regarding the boundary condition, a no-slip boundary condition is applied on the cylinder surface. In turn a Dirichler boundary condition is employed on the inlet is $u_1 = U_\infty \,\&\, u_2 = 0$, where at the outlet of computational area the boundary condition is $\frac{\partial u_1}{\partial x} = 0$. Whereas at the other lateral boundaries, a slip boundary condition is applied as: $\frac{\partial u_1}{\partial y} = 0 \,\&\, u_2 = 0$. To assure the mesh independency, a mesh refinement study is determined for the numerical resolution. Two cases of grid system are employed, named respectively as G1 and G2 has considered for the mesh independence study, the mesh generation parameters were shown in the table 2. At the period of mesh refinement, the time integration is performed by employing the predictor-corrector method, where the non-dimensional time integration interval is set to 0.001 for the grids G1&G2 respectively. In table 2, the global parameters of the calculated values for the elastically mounted circular cylinder are mentioned along with the percentage changes. From the table 2, is observed that the mesh changes from G1 to G2, it is evidently shows that the maximum deviation in the percentage change of 4.25% occurs in C_L for the case of elastically mounted circular cylinder with two interfering cylinders arranged in staggered configuration in upstream at different spacing ratios. Bestow the test results observed, at low Reynolds number the agreeable spatial and temporal resolutions for the simulations can be obtained by employing the grid G2 at $\Delta t = 0.001$.

The total mesh employed in the grid G2 for the case of an elastically mounted circular cylinder with two interfering cylinders arranged in staggered configuration in upstream at different spacing ratios consist of, total 65544 elements with 34342 nodes. The results of unsteady fluid flow over the elastically mounted circular cylinder in cross-flow direction are being used for validating the numerical accuracy.

TABLE 2. Grid independence test: A/D and C_L values for the elastically mounted circular cylinder at different interference conditions:

Interference condition	Grid System	Nodes on the cylinder	Elements	Nodes	A/D	C_L
Case I	G1	160	50162	25285	0.233	1.227
	G2	200	54598	28527	0.225 (1.12%)	1.235 (0.86%)
Case II	G1	180	52578	26039	0.261	1.236
	G2	240	65226	33065	0.265 (0.53%)	1.243 (0.72%)
Case III	G1	200	54768	26894	0.252	1.331
	G2	250	65431	34326	0.245 (0.78 %)	1.373 (3.59%)
Case IV	G1	200	54758	26886	0.180	1.310
	G2	250	65544	34342	0.160 (2.46 %)	1.363 (4.25%)

Results and discussion

A. Vibration amplitude

The responses of the test cylinder with and without interference conditions are observed to identify the maximum oscillatory amplitude ratio and its lock-in regime. Which were further analyzed to suppress the flow induced vibration fluctuation in the bluff bodies under various operating condition and geometrical arrangements. Whereas the responses observed in the each case are presented graphically as dimensionless oscillatory amplitude (A/D) versus reduced velocity (U/fD). The grid employed is tested for grid independency to obtain an optimized grid for the computational analysis. The response of circular cylinder is being studied under various operating conditions and geometric arrangements are mentioned below.

i. Single cylinder without interference,
ii. Cylinders arranged in tandem configuration by placing the interfering cylinder in downstream at different spacing ratios.
iii. Cylinders arranged in staggered configuration by placing the interfering cylinder in downstream at different spacing ratios.
iv. Cylinders arranged in staggered configuration by placing the interfering cylinders in upstream at different spacing ratios.

i. Response of an elastically mounted circular cylinder without interference

The flow characteristics of an elastically mounted test cylinder without interference conditions are shown in the Fig.2, 3, and 4.

In which it was observed that the reduced velocity crosses 4.5, where the cylinder exhibits perceptible amplitude of vibration. As the reduced velocity is increased further, the amplitude ratio reaches a maximum of 0.225 at a reduced velocity (U/fD) = 5.72. Further increase in the reduced velocity the amplitude decreases, where finally it is negligible, when it crosses the value of (U/fD) = 9. It clearly indicates that the lock-in regimes lays in the range of $4.5 \leq V_r \leq 9.0$.

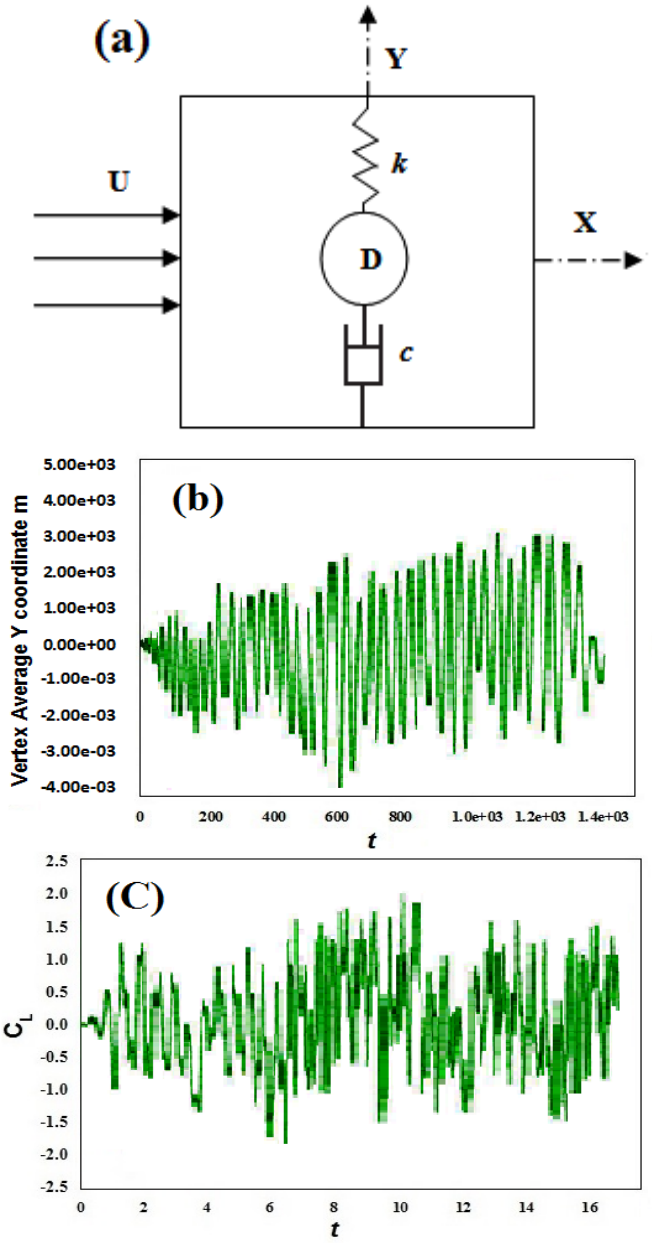

Fig 2: (a) Geometry of elastically mounted circular cylinder model in cross-flow without interference, (b) Displacement of cylinder and (c) lift coefficient

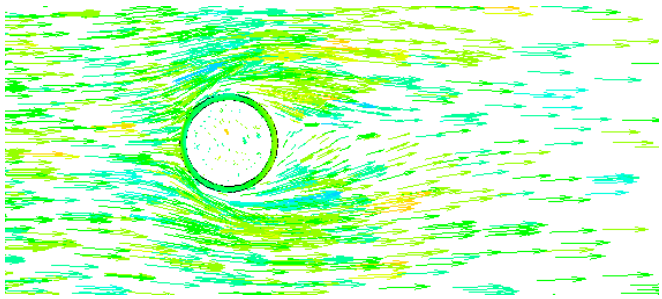

Fig 3: Velocity contours showing vortex shedding pattern for a single circular Cylinder without interference at different time intervals

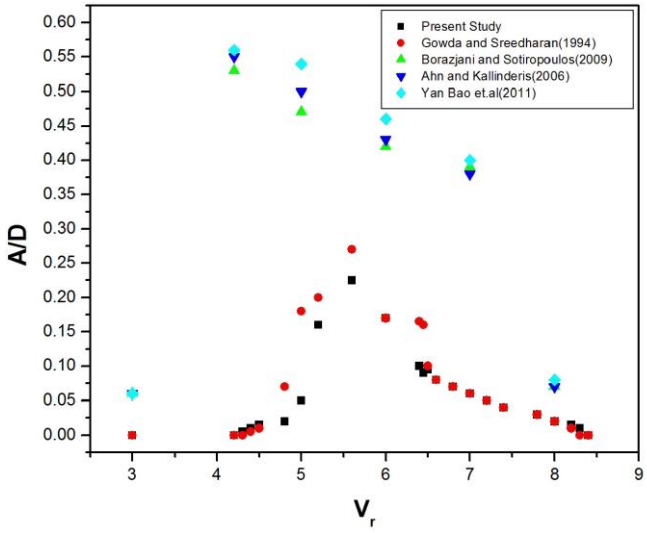

Fig 4: Response of an elastically mounted circular cylinder at without interference condition

ii Response of an elastically mounted circular cylinder with interference in tandem arrangement at different spacing ratios L/D = 2.0-4.0

The schematic diagram for the elastically mounted circular cylinder with interference in Tandem Arrangement at Different Spacing Ratios L/D = 2.0-4.0 is shown in Fig 5. The computation for the arrangement has been done at longitudinal pitch ratio of (L/D) = 2.0, 3.0 and 4.0 respectively. The vibration response of the cylinder in tandem arrangement for different longitudinal pitch is shown in the fig.6, where, the two cylinders are said to be in tandem when there is an off-set in the transverse direction.

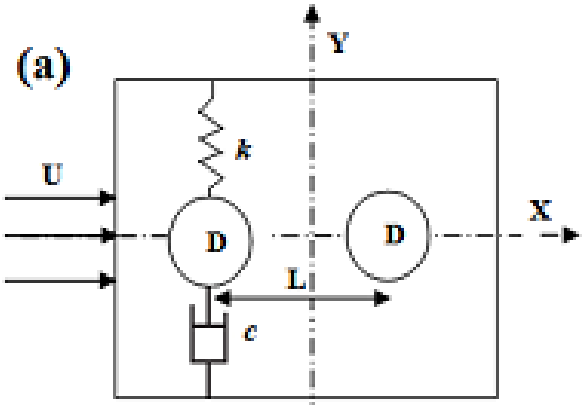

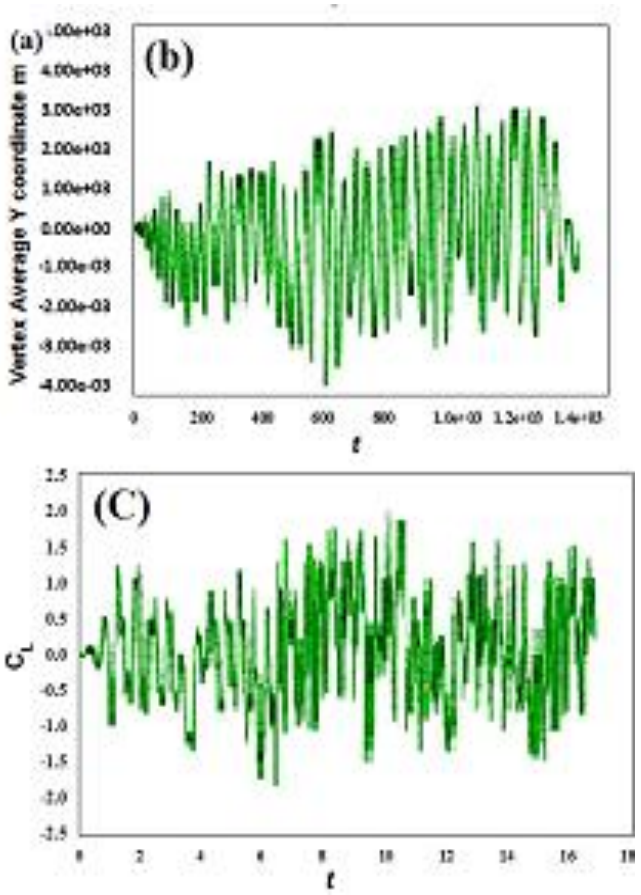

Fig 5: (a) Geometry of elastically mounted circular cylinder model in cross-flow with interference in downstream (b) Displacement of cylinder and (c) lift coefficient.

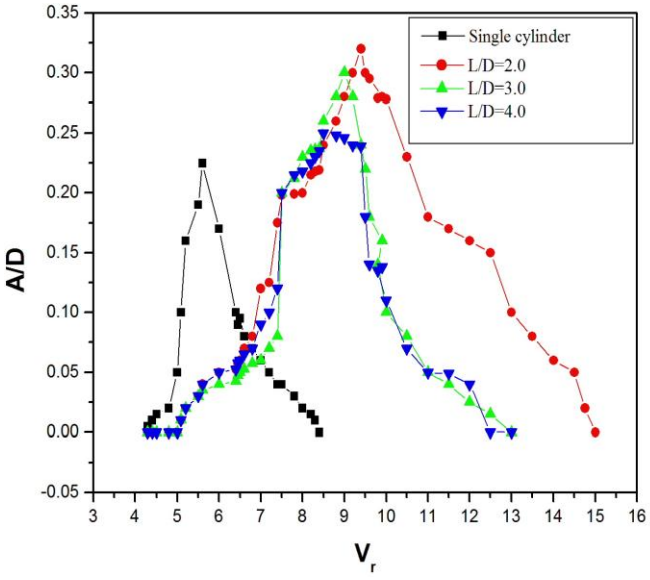

Fig 6: Response of an elastically mounted circular cylinder in tandem arrangement for different Longitudinal pitch (L/D = 2.0, 3.0 and 4.0)

iii. Response of an elastically mounted circular cylinder in staggered arrangement with two interfering cylinders in downstream at different spacing ratios L/D = 2.0-4.0 and T/D = 2.0-4.0.

The response of the test cylinder with interference cylinders arranged in staggered configuration for the gap ratios of L/D = 2.0 and T/D = 2.0 is shown in the Fig. 8, where the peak amplitude and lock-in regime of the test cylinder are larger than those of isolated cylinder. In this configuration when the reduced velocity is increased beyond the value of 5.0, the amplitude starts increasing and attains a peak at reduced velocity U/fD of 7.3. With further increase in the reduced velocity, the amplitude gradually reduces. The observed lock-in regime for this case lies in the range of $5.0 \leq V_r \leq 16.0$. In turn the response of the test cylinder for the same value of gap ratios is found to be similar. For further increase in transverse gap ratio T/D, the response of the test cylinder is not stable as evident from the jumps occurring in the lock-in range. Also, the vibration amplitude is supported relative to the isolated cylinder due to presence of the interfering Cylinders. From the response of Fig 9, it is observed that the test cylinder at the gap ratios L/D = 3.0 and T/D varied from 2.0 to 4.0. The vibration response of the test cylinder for the gap ratios L/D = 3.0 and T/D = 2.0 suddenly increases, when the reduced velocity reaches the value of 8.0. For further increase in the reduced velocity, the amplitude gradually decreases and it is very small for the values of U/fD more than 14.0. As the relative spacing between the interference cylinders in transverse direction is increased, the peak amplitude gradually decreases.

The response of the test cylinder with interference cylinders arranged in the gap ratios L/d = 4.0 and T/D = 2.0 is shown in the Fig. 10, where the oscillatory amplitude increases steeply when the value of U/fD crosses 6.5 and attains the peak at U/fD = 7.5. For further increase in the reduced velocity, the amplitude gradually decreases. The response of the test cylinder for the gap ratios L/D = 4.0 and T/D = 3.0 and 4.0 is quite similar to the previous case and it is observed that for further increase in transverse pitch of the interfering cylinders they do not have any influence on the test cylinder. In general, the response of the test cylinder with interfering cylinders in the downstream, the vibration amplitude is found to be higher for much closed spacing of the interfering cylinders in transverse direction.

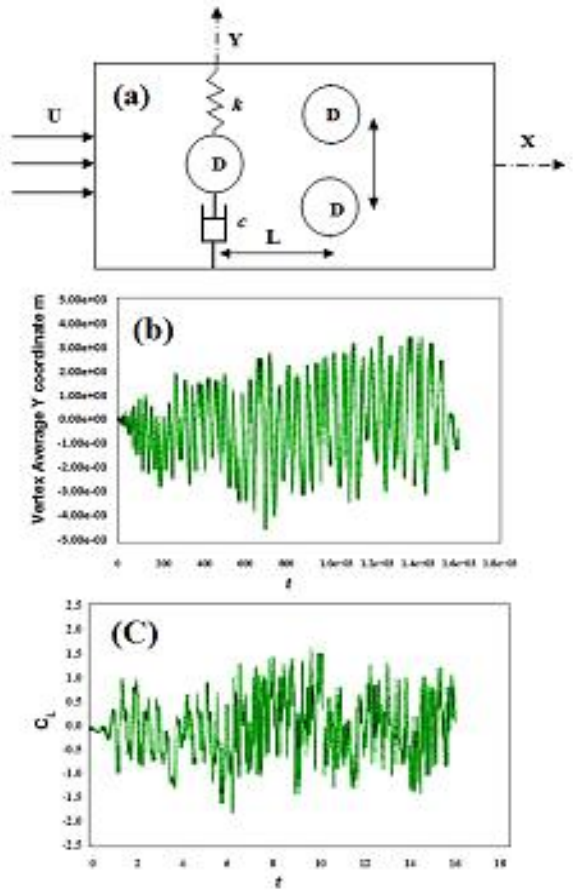

Fig 7: (a) Geometry of elastically mounted circular cylinder model in staggered arrangement with interference in downstream, (b) Displacement of cylinder and (c) lift coefficient.

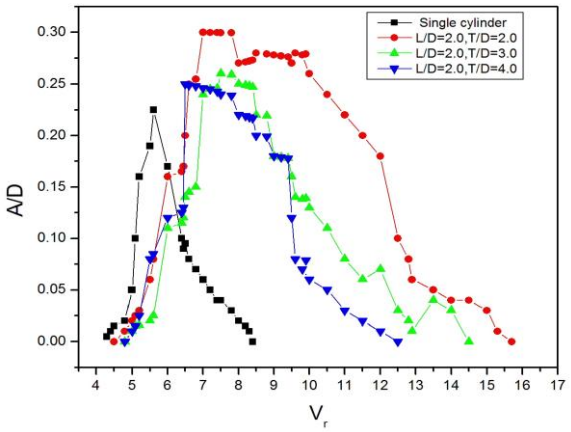

Fig 8: Response of an elastically mounted circular cylinder in staggered arrangement with two interfering cylinders in downstream at different spacing ratios (L/D = 2.0 and T/D=2.0, L/D=2.0 and T/D = 3.0, L/D = 2.0 and T/D = 4.0).

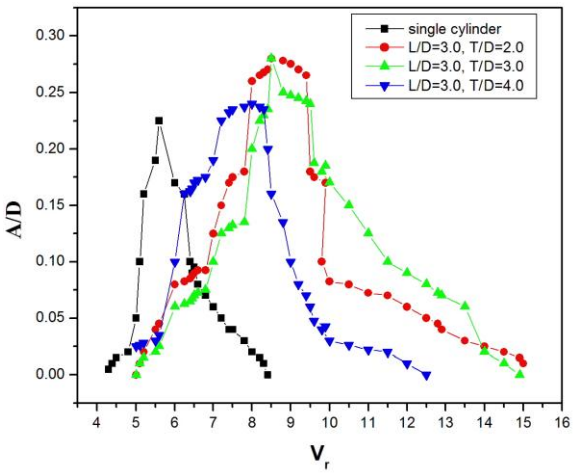

Fig 9: Response of an elastically mounted circular cylinder in staggered arrangement with two interfering Cylinders in downstream at different spacing ratios (L/D = 3.0 and T/D =2.0,L/D=3.0 and T/D = 3.0, L/D = 3.0 and T/D = 4.0).

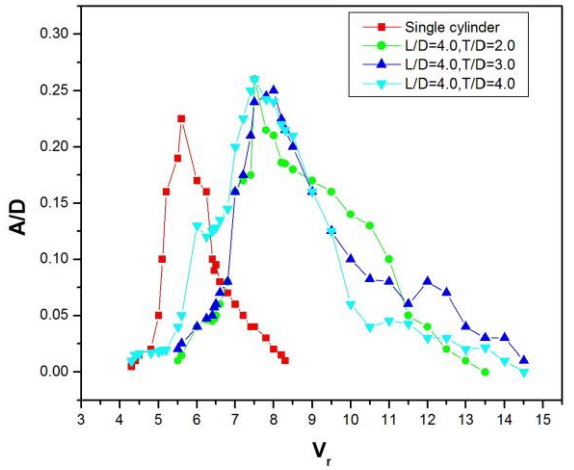

Fig 10: Response of an elastically mounted circular cylinder in staggered arrangement with two interfering Cylinders in downstream at different spacing ratios (L/D = 4.0 and T/D = 2.0, L/D=4.0 and T/D = 3.0, L/D = 4.0 and T/D = 4.0).

iv Response of an elastically mounted circular cylinder in staggered arrangement with two interfering cylinders in upstream at different spacing ratios L/D = 2.0-4.0 and t/d = 2.0-4.0.

The response of the test cylinder in staggered arrangement with two interfering cylinders in upstream at different spacing ratios is shown in the Fig. 11 to 14. The response of the test cylinder for the spacing ratios L/D = 2.0 and T/D = 2.0 is shown in the Fig 12, where the vibration starts at U/fD = 6.5 and it increases gradually up to U/fD = 12. For further increase in the flow velocity, there is no considerable change in the amplitude upto U/fD =17.5 and then it starts reducing. For further increase in spacing between the interference cylinders in the transverse direction, the peak amplitude is increased but the lock-in region is decreased. For the position of the interfering cylinders L/D = 2.0 and T/D=3.0, 4.0, the response of the test cylinder is quite similar. With increase in the transverse pitch of the interfering cylinders, the peak amplitude is lower than the previous case; however, it is higher than that of the isolated cylinder.

The response of the test cylinder for the spacing ratios L/D = 3.0 and T/D = 2.0 is shown in the Fig.13, in which the vibration excitation starts at the reduced velocity range of U/fD = 8.5 and it gradually increases with increase in reduced velocity. The maximum amplitude (0.25) occurs at U/fD = 21.0 and after that it starts decreasing. For position of the interfering cylinders at L/D and T/D = 3.0, the test cylinder vibration attains the peak value at U/fD 9.5 and gradually decreases with the increase in reduced velocity. It is observed that the peak amplitude decreases with the increase in the transverse pitch of the interfering cylinders. The response of the test cylinder for the spacing ratios of the interfering cylinders at L/D = 4.0 and T/D = 2.0 is shown in the Fig. 14, in which it is observed that the vibration excitation of the test cylinder is almost suppressed, i.e. the vibration amplitude is very small as compared to the response of the other configuration of the cylinder. Also, it is observed that the vibration amplitude gradually increases with the increase in transverse pitch of the interfering cylinders for L/D = 4.0. In general, when the interfering cylinders are placed in the upstream region of the test cylinder, the response is more remarkable than when they are placed in the downstream region. This feature is due the reason that when the interfering cylinders are placed in the upstream region, the vortices behind the interfering cylinders are shed in front of the test cylinder and could have the tendency to increase the lift force acting on the test cylinder. But, when the interfering cylinders are placed downstream of the test cylinder, the vortices behind the interfering cylinders do not have any effect on the test cylinder. The vibration of the test cylinder in this case is only due to vortices behind the test cylinder; but, in other case it is due to vortices behind the test cylinder and vortices behind the interfering cylinders. This may be the reason for getting high amplitude, when the interfering cylinders are placed upstream of the test cylinder.

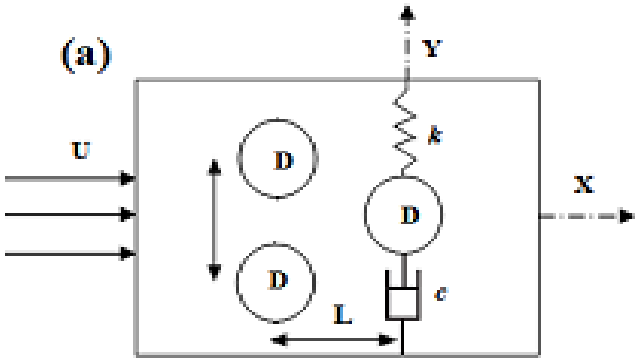

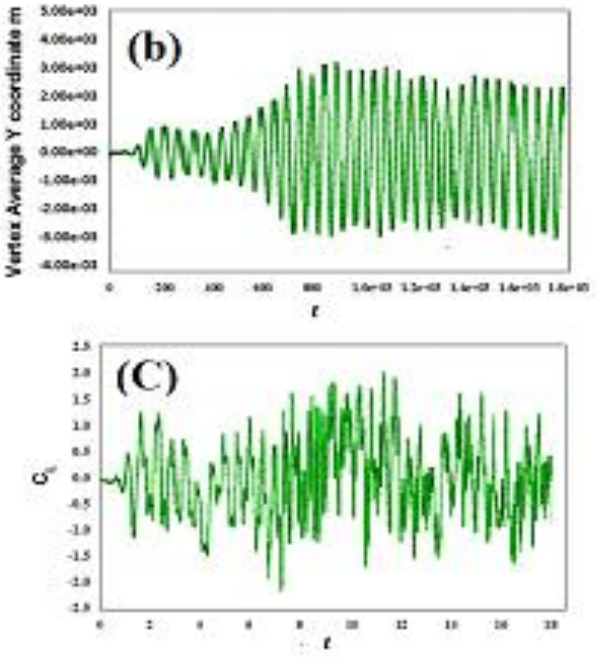

Fig 11 (a) Geometry of elastically mounted circular cylinder model in staggered arrangement with two interfering cylinders in upstream, (b) Displacement of cylinder and (c) lift coefficient.

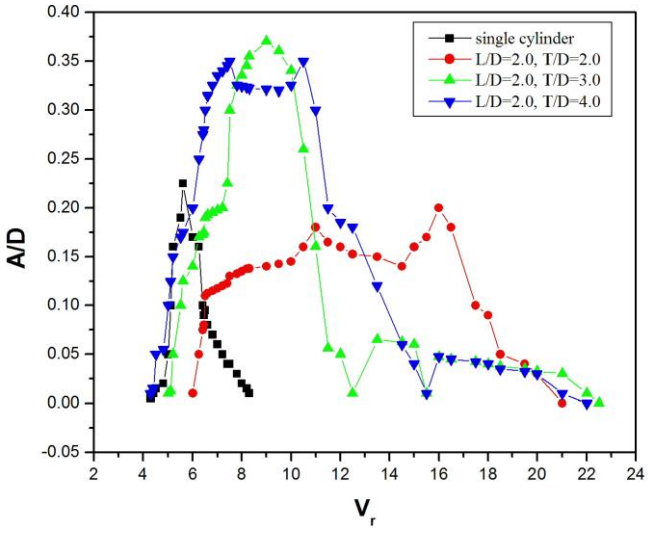

Fig 12: Response of an elastically mounted circular cylinder in staggered arrangement with two interfering Cylinders in upstream at different spacing ratios (L/D = 2.0 and T/D =2.0, L/D = 2.0 And T/D = 3.0, L/D = 2.0 and T/D = 4.0)

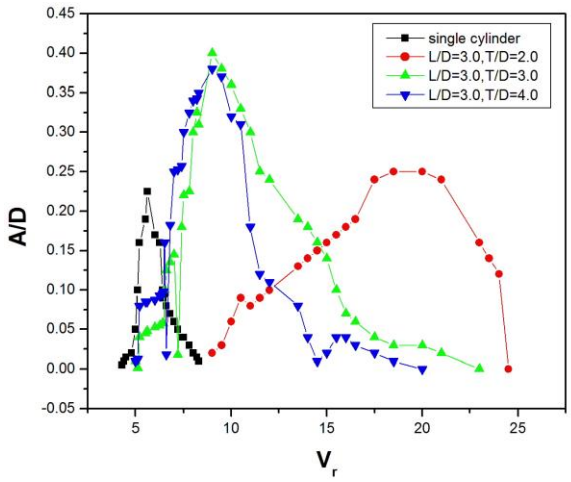

Fig 13: Response of an elastically mounted circular cylinder in staggered arrangement with two interfering Cylinders in upstream at different spacing ratios (L/D = 3.0 and T/D =2.0, L/D = 3.0 And T/D = 3.0, L/D = 3.0 and T/D = 4.0).

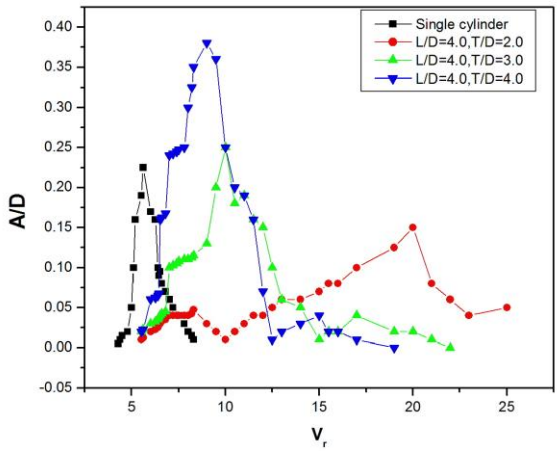

Fig 14: Response of an elastically mounted circular cylinder in staggered arrangement with two interfering Cylinders in upstream at different spacing ratios (L/D = 4.0 and T/D = 2.0, L/D = 4.0 And T/D = 3.0, L/D = 4.0 and T/D = 4.0).

B. Frequency

The frequencies of the induced vibration are obtained by employing the Fast Fourier Transform (FFT).

The variations in vibration frequency response of the elastically mounted circular cylinder in the cross flow direction with respect to the reduced velocity are shown in the Fig 15. For the gaping ratios of L/D=4.0, T/D=2.0 in the reduced velocity range of $8.5 \leq Vr \leq 21.5$, the vibration amplitude in the cross flow direction is observed to be Minimum, however the non-dimensional vibration frequency is close to 1. The frequencies indicated in Fig 15 are the peak frequencies of the suppressed cases of amplitude spectra based on the Fast Fourier Transform (FFT). Where, the frequencies observed for the other spacing ratios shows max vibration amplitude were not considered. For those cases,

beyond the lock-in region of the reduced velocity, the vibration Frequencies are found to be increasing with respect to increase in the reduced velocity. The result of current Numerical study is validated with the referenced studies at different interference conditions are given in the table 3 as follows. From the study, it is observed that the cylinder in staggered arrangement with two interfering cylinders in upstream at different spacing ratios exhibits the minimum oscillatory amplitude response (A/D) than the response of isolated cylinder observed in the Previous studies conducted by Ahn & Kallinderis(2006), Yan Bao et.al (2011), Borazjani & Sotiropoulos(2009), and Gowda & Sreedharan(1994).

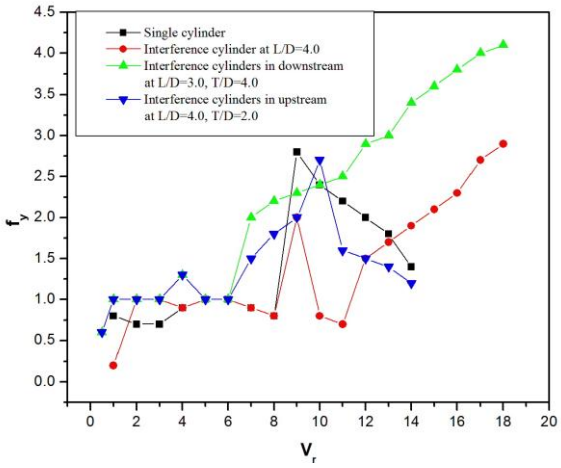

Fig 15: Variation of the vibration frequency in the cross-flow direction

TABLE 3. Validation of the numerical results with the experimental results

Interference conditions	Study	Longitudinal Pitch Ratio L/D	Transverse Pitch Ratio T/D	Oscillatory Amplitude Ratio A/D	Reduced Velocity (U/fD)	Lock in regime
Case I	Present study	-	-	0.225	6.0	$4 \le V_r \le 9$
	(1)	-	-	0.550	4.0	$3 \le V_r \le 6$
	(4)	-	-	0.560	4.0	$3 \le V_r \le 6$
	(8)	-	-	0.530	4.0	$3 \le V_r \le 6$
	(11)	-	-	0.270	6.0	$5 \le V_r \le 8.5$
Case II	Present study	4.0	-	0.265	5.0	$5 \le V_r \le 14.5$
Case III	Present Study	2.0	4.0	0.245	7.3	$5 \le V_r \le 16$
Case IV	Present Study	4.0	2.0	0.160	21.0	$8.5 \le V_r \le 21.5$

Conclusions

In order to predict the flow induced vibration excitation response of elastically mounted circular cylinder, a two dimensional numerically analysis is performed under with and without interference condition by arranging the cylinders in downstream and upstream respectively. Further, the observed results is compared with the previous study conducted by Ahn & Kallinderis(2006), Yan Bao et.al (2011), Borazjani & Sotiropoulos(2009), and Gowda & Sreedharan(1994).The results indicate that the vibration excitation with the increased oscillatory amplitude ratio is found to be more unstable and can grow into the strong fluctuation in the shear layer around the cylinder structures.

The following results have been observed in the course of this study:

1) The vibration response of the single cylinder in without interference condition, the result observed in the numerical analysis (i.e.) Maximum amplitude ratio A/D = 0.225 at reduced velocity of 5.72, is found to be almost equal to the experimental result of Maximum amplitude ratio A/D = 0.27 at reduced velocity as 6.0 respectively. Where the lock-in regime ($4.5 \le V_r \le 9.0$) also matches with the experimental work ($5 \le V_r \le 8.5$).
2) The vibration response of the test cylinder in tandem arrangement is found to be very high when the interfering cylinder is placed in the downstream close to the test cylinder. Also, the observed amplitude ratio (A/D = 0.265) is higher than that of the isolated cylinder (A/D=0.225). In turn, the vibration excitation of the test cylinder has been reduced, when the interfering cylinder is placed further away.
3) Among all the cylinder arrangements, the response of the cylinder in staggered arrangement with two interfering cylinders in upstream at L/D = 4.0 and T/D=2.0 spacing ratios, the oscillatory amplitude ratio is found to be minimum of A/D=0.160 at the lock-in regime of $8.5 \le V_r \le 21.5$ respectively. In turn, the observed result is compared with the previous studies that show that the vibration of the test cylinder is almost suppressed when the interfering cylinders placed in the upstream are very close for the same longitudinal pitch adopted as in the case of interfering cylinders placed in the downstream. However, the non-dimensional vibration frequency is observer to be nearer to 1.
4) The response of the test cylinder with interference cylinders arranged in staggered configuration is more remarkable when the interfering cylinders are placed at the upstream of the test cylinder than the interference cylinders at downstream. However, the vibration of the test cylinder is magnified when the interfering cylinders placed at the downstream is very close.
5) The lock-in regime is observed to be larger when the interfering cylinders are located at the upstream than the interfering cylinders that are in the downstream for same longitudinal and transverse pitch.

Finally, it is worth to mention that the implemented method is sufficiently applicable for the simulation of complex geometries. The presented results can be a good prediction of structural response of the elastically mounted circular cylinder at different interference conditions. Also, one can see that the oscillatory amplitude ratio (A/D) for the current study is lower

compared to the others. It should be noted that the current method employing the ALE based Finite Element method to solve the fluid flow characteristics, and hence, leads to produce more accurate results which is even more close to the real values.

Acknowledgement
Authors gratefully acknowledge the support of research grant (No.SB/FTP/ETA-389/2012) awarded by the Department of Science and Technology (DST), Government of India.

Nomenclature

D	Cylinder diameter
L	Centre-to-Centre longitudinal spacing (pitch)
L/D	longitudinal pitch ratio
Re	Reynolds number
A/D	Vibration Amplitude
T	Centre-to-Centre transverse spacing (pitch) (m)
T/D	Transverse Pitch Ratio
U	Free stream velocity
C_L	Lift coefficient
Y	Cross-flow coordinates
c	Damping Parameters
k	Stiffness
f_y	Vibration Frequency
V_r	Reduced velocity
τ_{ij}	Stress tensor
M	Mass matrix
G	Gradient matrix
a	acceleration vector
v	Material velocity vector
$\hat{v}$	Mesh velocity vector
p	Pressure vector

Reference

[1] Ahn, H.T., and Kallinderis, Y., Strongly coupled flow/structure interactions with a geometrically conservative ALE scheme on general hybrid meshes, Journal of computational Physics, 2006, 219, 671-696.

[2] Ajith Kumar, R., Gowda, B.H.L. Flow-induced vibration of a square cylinder without and with interference, Journal of Fluids and Structures, 2006, 22, 345-369.

[3] Ajith Kumar, R., Sugumaran, V., and Gowda, B.H.L., Sohn, C.H, Decision tree: A very useful tool in analyzing flow-induced vibration data, Mechanical Systems and Signal Processing. 2008, 22, 202-216.

[4] Bao, Y., Zhou, D., and Tu, J., Flow interference between a stationary cylinder and an elastically mounted cylinder arranged in proximity, Journal of Fluids and Structures, 2011, 27, 1425-1446.

[5] Blevins, R.D. Flow-Induced Vibration, second ed. Van Nostrand Reinhold, New York 1990.

[6] Biswas, Saroj K., Ahmed, N. U. Optimal Control of Flow-Induced Vibration of Pipeline, Dynamics and Control, 2001, 11, 187-201.

[7] Borazjani, I., Sotiropoulos, F., Vortex-induced vibrations of two cylinders in tandem arrangement in the proximity-wake interference region, Journal of Fluid Mechanics, 2009, 621, 321-364.

[8] Cheng, L., Zhou, Y. Surface perturbation technique for flow-induced vibration and noise control, Journal of Sound and Vibration, 2008, 310, 527-540.

[9] Gelbe, H., Jahr, M., Schroder, K., Flow-induced vibrations in heat exchanger tube bundles, Chemical Engineering and Processing, 1995, 34, 289-298.

[10] Gowda, B. H. L. and Sreedharan, V., Flow-induced oscillations of a circular cylinder due to interference effects. Journal of Sound and Vibration, 1994, 176**,** 497-514.

[11] Hiejima, S., Nomura, T., Kimura.K., and Fujino, Y., Numerical study on the suppression of the vortex induced vibration of a circular cylinder by acoustic excitation, Journal of Wind Engineering and Industrial Aerodynamics, 1997, 67 & 68, 325-335.

[12] Hyun-Boo Lee, Tae-Rin Lee, and Yoon-Suk Chang. Numerical simulation of flow-induced bidirectional oscillations" Journal of Fluids and Structures, 2013, 37, 220-231.

[13] Jubran, B. A., Hamdan, M. N., and Shabaneh, N. H. Wavelet and chaos analysis of flow induced vibration of a single cylinder in cross-flow, International Journal of Engineering Science, 1998, 36, 843±864.

[14] Kang, H.S., Song, K.N., Kim, H.K., and Yoon, K.H. Axial-flow-induced vibration for a rod supported by translational springs at both ends, Nuclear Engineering and Design, 2003, 220, 83-90.

[15] K.Karthik Selva Kumar, K.Aruna Devi, and L.A. Kumaraswamidhas, SPSS: A Data mining tool for analyzing the results of flow induced vibration excitation in an elastically mounted circular cylinder at different interference conditions, Applied Mechanics and Materials, 2014, 592-594, 2086-2090.

[16] Karthik Selva Kumar. K and Kumaraswamidhas. L.A, Numerical Study on Fluid Flow Characteristics Over the Side-By-Side Square Cylinders at Different Spacing Ratio, International Review of Mechanical Engineering, 2014, 8, 962-969.

[17] K.Karthik Selva Kumar, and L.A. Kumaraswamidhas, (2014) "A Study on Flow Induced Vibration Excitation in Solid Square Structures", International Journal of Mechanical & Production Engineering Research and Development, 2014, 4(4), 15-22.

[18] Karthik Selva Kumar K., and Kumaraswamidhas L. A. Experimental investigation on flow induced vibration excitation in the elastically mounted circular cylinder in cylinder arrays. Fluid Dynamic Research, 2015, 47, 015508.

[19] Karthik Selva Kumar K., and Kumaraswamidhas L. A. Experimental investigation on flow induced vibration excitation in the elastically mounted square

cylinders. Journal of Vibroengineering, 2015, 17, 468-477.

[20] Karthik Selva Kumar K., and Kumaraswamidhas L. A. Experimental and Numerical Investigation on Flow Induced Vibration Excitation In Engineering Structures: A Review, International Journal of Applied Engineering Research, 2015, 10(15), 35971-35991.

[21] Korkischko, I., and Meneghini, J.R. Experimental investigation of flow-induced vibration on isolated and tandem circular cylinders fitted with strakes. Journal of Fluids and Structures, 2010, 26, 611-625.

[22] Ostanek, J., K., and Thole, K, A. Wake development in staggered short cylinder arrays within a channel, Exp in Fluids, 2012 53, 673-697.

[23] Perotin, L., and Granger, S. An Inverse Method For The Identification Of A Distributed Random Excitation Acting On A Vibrating Structure Part 2: Flow-Induced Vibration Application, Mechanical Systems and Signal Processing, 1999, 13 (1), 67-81.

[24] Pettigrew, M.J., Taylor, C.E., Fisher, N.J., Yetisir, M., and W. Smith B.A. Flow-induced vibration: recent findings and open questions, Nuclear Engineering and Design, 1998, 185, 249±276.

[25] Sang-Nyung Kim and Yeon-Sik Cho. The Analysis of Flow-Induced Vibration and Design Improvement in KSNP Steam Generators of UCN #5, 6, KSME International Journal, 2004, 18(1), 74-81.

[26] Shiels, D., Leonard, A., and Roshko, A. Flow-Induced Vibration of a Circular Cylinder at Limiting Structural Parameters, Journal of Fluids and Structures, 2001, 15, 3-21.

[27] Wu, W., Yuan, J., and Cheng, L. Multi-high-frequency Perturbation effects on flow-induced vibration control, Journal of Sound and Vibration, 2007, 305, 226-242.

[28] Zhou, Y. Vortical structures behind three side-by-side cylinders, Experiments in Fluids, 2003, 34, 68-76.